Using Trajectory Smoothness Metrics to Identify Drones in Radar Track Data

Sandip Roy, David Petrizze, and Logan Dihel
Washington State University, Pullman, WA 99163

Mengran Xue
Raytheon BBN Technologies, Columbia, MD 22104

Chester Dolph, Henry Holbrook
National Aeronautics and Space Administration, Hampton, VA 23681

Abstract **–** The identification of unmanned aircraft systems (UAS) using trajectory data is considered. Specifically, a number of smoothness metrics are proposed, which can be used to distinguish UAS from other aerial objects even when they are engaged in accelerative maneuvers (non-constant-velocity flight). The metrics are evaluated on a data set from a UAS sense-and-avoid field test, which contains track data of aerial objects recorded by a vehicle-board radar system during a flight test. The metrics are found to effectively differentiate UAS from other objects such as birds for this data set. In addition, an initial statistical performance analysis of one of the smoothness metrics is undertaken, using 15 data sets deriving from multiple flight tests. The smoothness metric is shown to identify the target UAS with 95% accuracy (95% true positive rate), while achieving a false positive rate of less than 9%.

I. Introduction

There is an increasing need for technologies that can identify small- to medium- sized unmanned aircraft systems (UAS), colloquially known as drones, based on signatures in sensor measurements. Specifically, UAS identification is a critical component in ground-based CounterUAS systems, which are tasked with monitoring and preventing UAS intrusions to security-sensitive facilities like ports, prisons, and sports venues. UAS identification is also needed for sense-and-avoid systems deployed on both unmanned and manned aerial vehicles, which are responsible for recognizing and avoid potential collisions. Vehicle- and ground- based UAS-identification systems are of use to military stakeholders, for both defensive and offensive operations. A key challenge in these applications is to identify UASs with high sensitivity and specificity. In particular, techniques are needed which provide alarms for UAS intrusions with high confidence, while also excluding other aerial objects such birds.

UAS identification using signatures in radio-frequency (RF) signals has been thoroughly researched [1]. A number of relatively mature technologies which use RF signatures are available on the market, at a reasonable cost. These technologies nominally are able to detect radio-controlled drones with high sensitivity and specificity. However, RF-based techniques cannot be used for UASs that are not radio controlled, including autonomous, GPS-based, or cellular-network-based UASs. In addition, RF-based UAS identification technologies are spoofable, do not work when mounted on platforms with separate RF communication needs, and typically cannot distinguish between different types of UASs. A few studies have also attempted UAS identification based on comparison of images or videos with labeled recordings [2]. This approach can allow for detection of non-radio-controlled drones but requires exhaustive archiving of drone images, and tends to be sensitive to the drone configuration and distance from the imaging device. Typically, high-resolution imaging is also needed, which may be costly.

Very recently, a few research groups have pursued UAS identification from trajectory signatures obtained from video data [3-5]. The basic concept is that ambient fluctuations in an aerial object's trajectory give an indication of the type of object (e.g., drone vs bird), as they depend on the inertial characteristics and control mechanisms of the object. This concept has been leveraged in two different ways to UAS drone identification algorithms. The first approach is based on defining a set of intuitive features that characterize the ambient fluctuations, and then applying

a machine learning algorithm to develop a classifier for the object type, hence distinguishing UASs from other objects. The second approach is based on abstracting the aerial object classification problem to a statistical hypothesis testing problem for a feedback-controlled inertial system, and using this abstraction to determine features for classification. Learning and identification are then pursued in this feature space. Both approaches have been tested on field data, and show promise to enable high sensitivity and specificity identification. Broadly, these trajectory-based approaches are appealing because they are generic, difficulty to spoof, trainable in an unsupervised way, and potentially can be implemented using low-cost imaging platforms.

While the approaches developed for trajectory-based UAS identification appear to be promising, one complication in their use is that their performance may degrade if the UAS being identified is accelerating rather than engaging in straight-line constant-velocity flight. This is because the features used for identification essentially aim to measure the envelope of spread around a straight line flight path. Thus, if a UAS (or other flying object) is engaging in a complex maneuver, feature values may reflect both the nominal flight behavior and its low level trajectory fluctuations, introducing error into the measures. This complication motivates exploration of alternative or additional features for identifying drone flights from trajectory data.

Conceptually, low-level ambient fluctuations in aerial object trajectories should be differentiable from object maneuvers, given that: 1) fluctuations typically persist at shorter temporal scales and distances compared to deliberate maneuvers and 2) maneuvers often exhibit organized patterns which are atypical in ambient fluctuations. To facilitate identification from ambient fluctuations, features or metrics are therefore needed which only measure the characteristics of the fluctuations and filter out the (unknown) maneuvers. In fact, researchers in signal analytics have defined features and approaches for measuring such low-level fluctuations while ignoring persistent trends in time-series metrics [6]. These features/computations are broadly termed as *smoothness metrics* for a signal. The purpose of this study is to explore whether a set smoothness metrics can help to distinguish drones from other flying objects using trajectory data.

II. Motivation and Approach

We are interested in distinguishing aerial objects based on recordings of their trajectories, as obtained from a radar/imaging system or other sensor. Broadly, the sensing system is assumed to provide samples of the object's trajectory in space, at a specified sampling rate. For some sensing systems (e.g. advanced radar systems), the full trajectory in three dimensions may be recorded. For other sensors (e.g. cameras), only a projection of the trajectory in a lower dimension may be captured. Our objective is to distinguish the type of the aerial object (e.g., whether it is a bird or a UAS, or the type of UAS) from the trajectory recordings. We are interested in distinguishing the object type using short-duration trajectories, so as to allow for fast identification in real-time applications.

To motivate an approach for distinguishing aerial objects from trajectory data, it is helpful to abstractly model the physical processes defining an object's flight. Since we seek for a detector that uses trajectory data, we focus on modeling the ambient trajectory fluctuations of objects in flight: the main idea is that aerial objects aim to follow desired trajectories, but shake or wobble away from these trajectories in distinct ways because they have different inertial responses to ambient stimulation/noise (i.e., wind and other environmental factors). To capture these characteristics, we formally consider N types of aerial objects, labeled $i = 1, \dots, N$. Each object $i = 1, \dots, N$ is represented as being governed by an intertial dynamics, however with a different mass $m_i$and damping/friction coefficient b_i. Each object type is modeled as using a different feedback controller to follow a desired (time-varying) reference trajectory in each Cartesian coordinate direction (say $r_x(t)$ in the x-coordinate direction). The objects are additionally actuated by stochastic additive environmental disturbances in each coordinate direction (say $w_x(t)$ in the x-coordinate direction). The measurement device is assumed to collect regularly-spaced samples of the three-dimensional trajectory, or projections thereof in lower-dimensional space, perhaps with some corruption due to environmental noise. In general, we note that both object position and velocity measurements may be available, or velocity measurements may be estimated from the position measurements. We use the notation $\boldsymbol{y}$[k] for the vector of sampled trajectory measurements of an object at a time step k. The measurements are assumed to be taken over a period of time (say time steps $k = 0, \dots, k_f$), while the object is in the measurement device's field of view.

Our interest lies in distinguishing the object type from all or part of the measurement sequence $\boldsymbol{y}$[k]. This problem can be viewed formally as a statistical hypothesis testing or detection problem. The hypothesis-testing problem is complicated by the fact that both the object models and the input signals, including the reference trajectory and environmental disturbances, are unknown to the detector. In our prior work [4], we determined the maximum *a posteriori* probability (MAP) detector, for the special case that the reference signal is linear (i.e. the object is following

a constant-velocity path), the environmental disturbance is Gaussian white noise, and the measurement noise is negligible. In this special case, the MAP detector only depends on two sufficient statistics – the sample variance or second moment of the mean-removed velocity measurement sequence ($s_0 = \frac{1}{k_f}\sum_{k=0}^{k_f-1} \boldsymbol{v}^T[k]\,\boldsymbol{v}[k]$), and the first tap in the sample autocorrelation of the measurements ($s_1 = \frac{1}{k_f-1}\sum_{k=0}^{k_f-2} \boldsymbol{v}^T[k+1]\,\boldsymbol{v}[k]$), where we have used the notation $\boldsymbol{v}[k]$ for the mean-removed velocity measurements. The optimal detector compares a linear combination of the two statistics to thresholds to determine the object type, where the weightings of the statistics and the thresholds depend on object-model constants (mass, damping, control gains). We showed in further work that the detector parameters can be learned from relatively-sparse archived trajectory data [5]. Hence, a data-only solution which consists of a learning module and a real-time detector can be developed. The methodology has been tested successfully on both synthetic and field data, and an error probability computation for the optimal detector has also been undertaken.

A key limitation of our prior approach is that the reference trajectories of the objects are assumed to be linear, i.e. the object is assumed to engaged in constant-velocity flight during the measurement period. However, aerial objects including UASs and birds often may be engaged in accelerative maneuvers (e.g., banking or curving flight) while they are measured. Further, for measurements taken from a mobile platform, measured trajectories will not be constant-velocity if either the measurement platform or the measured object is engaged in an accelerative maneuver. As an example, radar-measurements from a vehicle-board platform capture a UAS engaged in curved flight in Figure 1, see Sections IV and V for further details about the experimental data set). For this data, direct application of the MAP detector described above does not work well, as the sufficient statistics are corrupted by the curvature of the UAS. In particular, the sufficient statistics are much larger than their expected values, as the UAS's trajectory appears to vary relative to a constant-velocity reference. Thus, the technique for distinguishing object types needs to be modified to account for the possibility of curved flight.

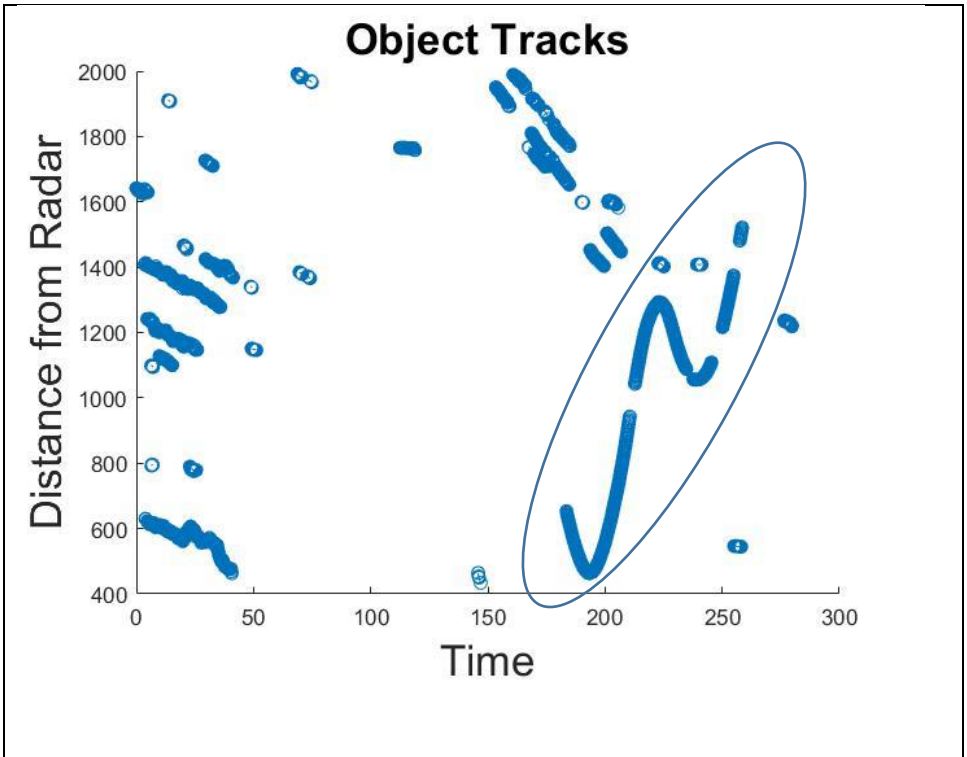

Figure 1: Aerial object tracks detected by a radar mounted on a UAS during a flight test are shown. Tracks corresponding to a second UAS in the field of view of the radar are shown. The second UAS is maneuvering during the period, but nevertheless has a smooth trajectory.

We thus aim to develop methods for distinguishing aerial objects from trajectory data, which account for the possibility of non-constant-velocity flight. In this initial study, we do so by developing simple heuristics for aerial-

object detection which incorporate trajectory curvature. Our methodology is primarily based on the following concept: broadly, the desired flight paths or reference trajectories of objects, while non-constant, are 1) sparse in a Fourier or polynomial basis and 2) primarily made up of low-frequency components. This suggests the possibility for using signal processing measures of *smoothness*, which capture the complexity or extent of local variations in a signal around a low-frequency trend, to determine aerial-object type. In particular, we anticipate that a number of directly-calculated smoothness metrics can be used to categorize object types. Alternately, it may be possible to estimate smoothness and hence categorize objects, by first fitting a low-dimensional and low-frequency curve to the data and then comparing the signal to the fit. Here, we explore categorization of aerial objects from trajectory data using such smoothness metrics.

The smoothness metrics are defined in the following Section III. Then, the application of the metrics to categorize aerial objects is undertaken for an example data set obtained from field measurements in Section IV. An initial performance analysis of a detector across multiple field data sets is presented in Section V.

III. Smoothness Metrics and Heuristics

Smoothness metrics in our study are computed from a scalar function of the measurement data, such as the radial distance of the object from the radar, the position in one coordinate direction, or the heading. In general, we use the notation $z[k] = f(\boldsymbol{y}[k])$ for the scalar function of the measurements that is used for calculating smoothness metrics, and refer to it as the *detection variable*.

A simple metric for smoothness is the sample variance of the one-step difference in the detection variable computed over a time interval, which captures whether the detection variables follows a linear trend over the interval. Mathematically, this smoothness metric $M(1)$ can be computed as:

$$M(1) = \frac{1}{T} \sum_{k=k_0}^{k_0+T-1} (z(k+1) - z(k) - q)^2$$

where

$$q = \frac{1}{T} \sum_{k=k_0}^{k_0+T-1} z(k+1) - z(k)$$

and where T is the time horizon over which the sample statistics are computed, k_0 is the initial time from which data is used for the computation, and q is the sample mean of the first difference signal. Small values of the metric $M(1)$ correspond to a high smoothness, while larger values are indicative of a rough or less smooth signal. Selecting the time horizon T for the smoothness calculation entails a tradeoff: longer time horizons yield more robust statistics, but also require a longer delay in real-time processing and make the statistics susceptible to nonlinear trends in the detection variable.

The metric $M(1)$ is an absolute measure of spread in the first-difference signal, and does not consider the relative magnitude of the spread compared to the size or amplitude of the first difference signal. An alternate smoothness metric of interest is one that scales the spread metric by the amplitude of the first-difference signal. Formally, an alternate smoothness metric $M(2)$ can be defined as:

$$M(2) = \frac{M(1)}{c}$$

where

$$c = \frac{1}{T} \sum_{k=k_0}^{k_0+T-1} |z(k+1) - z(k)|$$

The metric $M(2)$ scales for the absolute amplitude of the first difference signal in determining smoothness. Again, small values of the metric correspond to high smoothness, while large values indicate low smoothness.

Although the metric $M(2)$ provides an apt indicator for smoothness for fast-changing signals, it may give deceptive results when the first-difference signal has small amplitude. In this case, the metric $M(2)$ may become large even if the signal does not exhibit much variation, while visual inspection would suggest that the signal is smooth. From another viewpoint, interpreting smoothness as a relative measure is sensible for sufficiently fast-changing signals, but not for very slowly changing (small first-difference) signals. One simple way to define a metric that differentiates between the two regimes is to combine the two metrics $M(1)$ and $M(2)$, In particular, the following metric $M(3)$ can be defined:

$$M(3) = \min\left(M(1), pM(2)\right)$$

where p is a positive constant. The metric $M(3)$ captures variability relative to the amplitude of the first-difference signal provided that the amplitude is sufficiently large, but reverts to an absolute measure for small-amplitude first-difference signals.

Beyond the above direct computations, smoothness can alternately be defined from the residual, upon removal of low-frequency sinusoidal or polynomial signals from the detection variable signal $z[k]$. In particular, removal of low-frequency sinusoids can be achieved by applying a high-pass filter to the signal $z[k]$ over an interval (say $k_0, \dots, k_0 + T - 1$), yielding the filtered or residual signal $z_{HP}[k]$. Smoothness can then be defined as the sample variance of the signal $z_{HP}[k]$:

$$\boldsymbol{M(4) = \frac{1}{T} \sum_{k=k_0}^{k_0+T-1} \left(z_{HP}[k]\right)^2}$$

where we note that the signal mean can be assumed to be zero since it is the result of a high-pass filtration. Alternately, the smoothness can be computed by finding the best-fit polynomial of degree w for $z[k]$ over an interval (say $k_0, \dots, k_0 + T - 1$), and then subtracting this best-fit polynomial from $z[k]$ to get a residual signal $s[k]$. The smoothness can the be defined as the second moment of this residual:

$$M(5) = \frac{1}{T} \sum_{k=k_0}^{k_0+T-1} \left(s[k]\right)^2$$

The metrics $M(4)$ and $M(5)$ can also be normalized by the absolute amplitude or energy in the first-difference signal, to obtain a relative metric.

IV. Evaluation of the Smoothness Metrics on an Example Data Set

The proposed smoothness metrics were evaluated on a test data set which includes trajectories of a small UAS in flight, along with trajectories or other aerial objects. The test data set derives from the National Aeronautics and Space Administration's RAAVIN (Radar on Autonomous Aircraft to Verify ICAROUS Navigation) flight test [3,7,8]. The flight test was conducted to assess the ICAROUS (Independent Configurable Architecture for Reliable Operations of Unmanned Systems) software system, which was developed by NASA to enable sense-and-avoid for unmanned traffic management (UTM). The flight test was conducted using a lightweight metamaterials-based radar mounted underneath a small UAS (henceforth referred to as the "ownship"), which obtained location and velocity measurements for aerial objects in its field of view including other UAS, manned aircraft, and birds. The flight test demonstrated that the radar routinely alarmed a substantial number of objects in flight, beyond the target UAS (henceforth called "targetship") which was the object of the flight test. Thus, flight test personnel recognized the need to distinguish small/medium UAS (here the targetship) from other objects in flight, so as to allow efficient functioning of the ICAROUS navigation system. This has initiated a sequence of studies on target differentiation based on ambient trajectory data, as obtained by the radar system (e.g. [3]). Our effort here continues this track of work, using the same data sets from the RAAVIN flight test.

Further details about the ICAROUS navigation system, the RAAVIN flight test, the ownship (including the radar mount), and the targetship can be found in prior work [2,7,8]. Relevant to our development here, a number of different flight tests were conducted. For each flight test, the radar system produced recordings of location and velocity tracks (trajectories) for detected objects, at a rate of 9Hz. For the study discussed in this section, the track data set associated with one of the flight tests was used to evaluate the proposed smoothness metrics. For this test data set, 40 tracks of longer than 1 s were recorded, of which 1 track corresponded to the targetship and the remaining tracks were of other objects in flight (e.g. birds). Tracks exceeding 1s in duration are shown in Figure 2 below. Visual inspection suggests that the targetship's tracks indeed appear smooth compared to the other tracks.

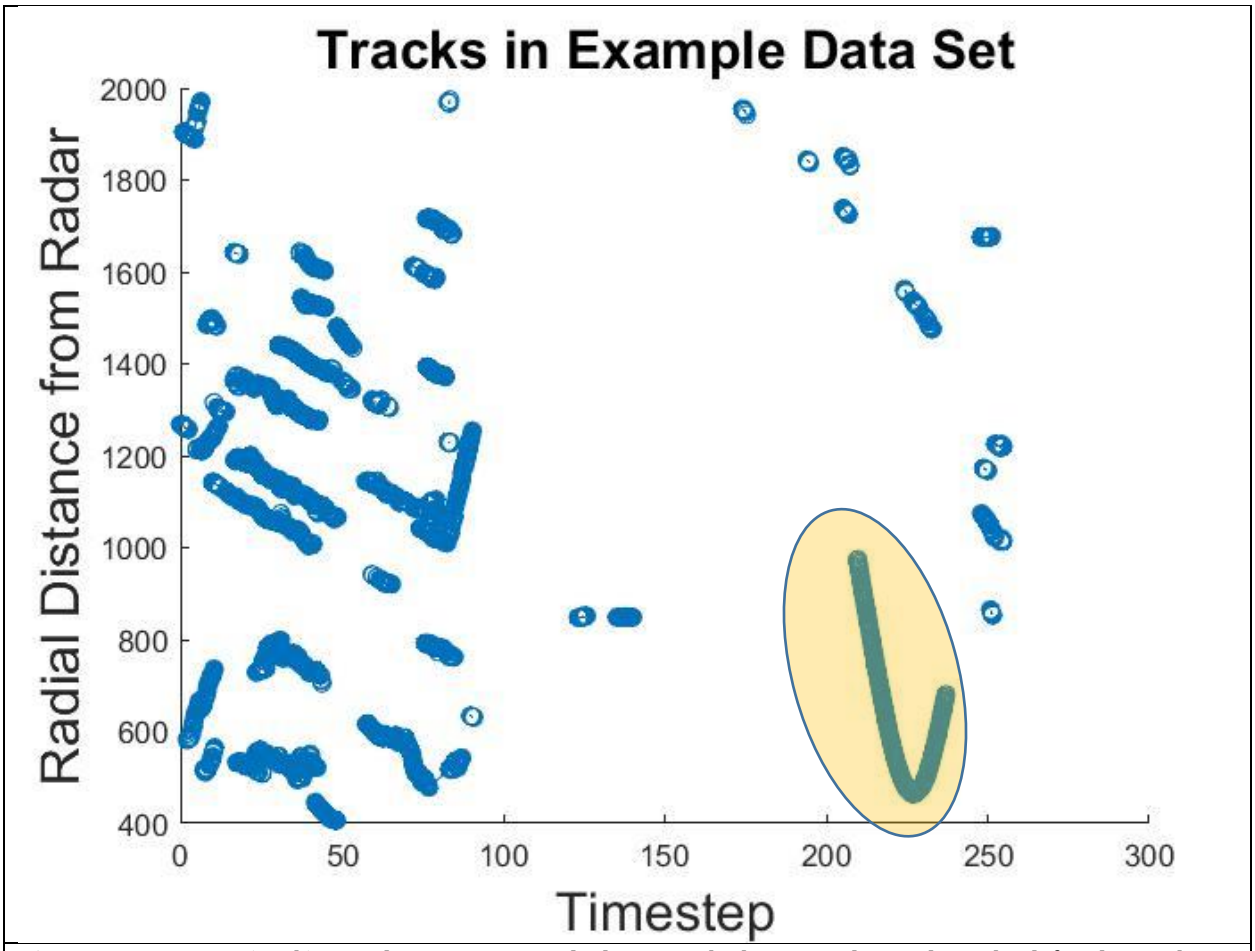

Figure 2: Trajectory (track) recordings in an example data set, which was used to evaluate the defined smoothness metrics. The figure shows the radial distance of each tracked object from the radar. The targetship's track, highlighted with an orange oval, visually appears to be smooth.

We have undertaken several analyses of the test data set, to study the smoothness metrics defined in Section III. First, each metric was computed for all tracks of sufficient duration, using 1s of data starting from 0.3s after the beginning of the track. The radial distance of the object from the radar was used as the For the metric M(1), the targetship was found to have a metric value of M(1)=0.20. This was substantially smaller than the average metric value of M(2)=1.17 for other tracks. However, 6 of the other tracks were found to have metric values M(1) less than that of the targetship. These six tracks along with the targetship's track are shown in Figure 3. The metric is seen to be small for other slow-changing, short-duration tracks. For the metric M(2), the targetship was found to have a metric value of M(2)=0.042. The metric value for all other tracks was found to be M(2)>0.058, and hence a threshold of 0.05 achieves a perfect classifier for this metric; this classification is shown in Figure 4. The average metric value for the other tracks was M(2)=0.97, indicating a large difference between the targetship track and most other tracks. For this example, metric M(3) would trivially also distinguish the targetship's track for sufficiently large p, hence details are obtained; the metric M(3) may be of importance if the targetship's track is itself slow moving. To compute measure M(4), a five-point finite-impulse-response high-pass filter with a triangle-type shape was applied to the data. The metric was then computed, using a normalization based on the average absolute value of the first-difference signal. The metric M(4) for the targetship track was found to be M(4)=0.0429, while the metric values for all other tracks were found to satisfy M(4)>0.11. Thus, a perfect classifier was also achieved with the metric M(4), based on a threshold of 0.075. Finally, the metric M(5) was computed based on a cubic-polynomial fit. The metric was then found as the energy in the residual, normalized by the average absolute value of the first-difference signal. The metric for the targetship was found to be M(5)=0.071, while the metric values for all other object tracks were found to satisfy M(5)>0.11. Thus, the metric M(5) also was able to exactly differentiate the targetship from other tracks with a threshold of M(5)=0.09.

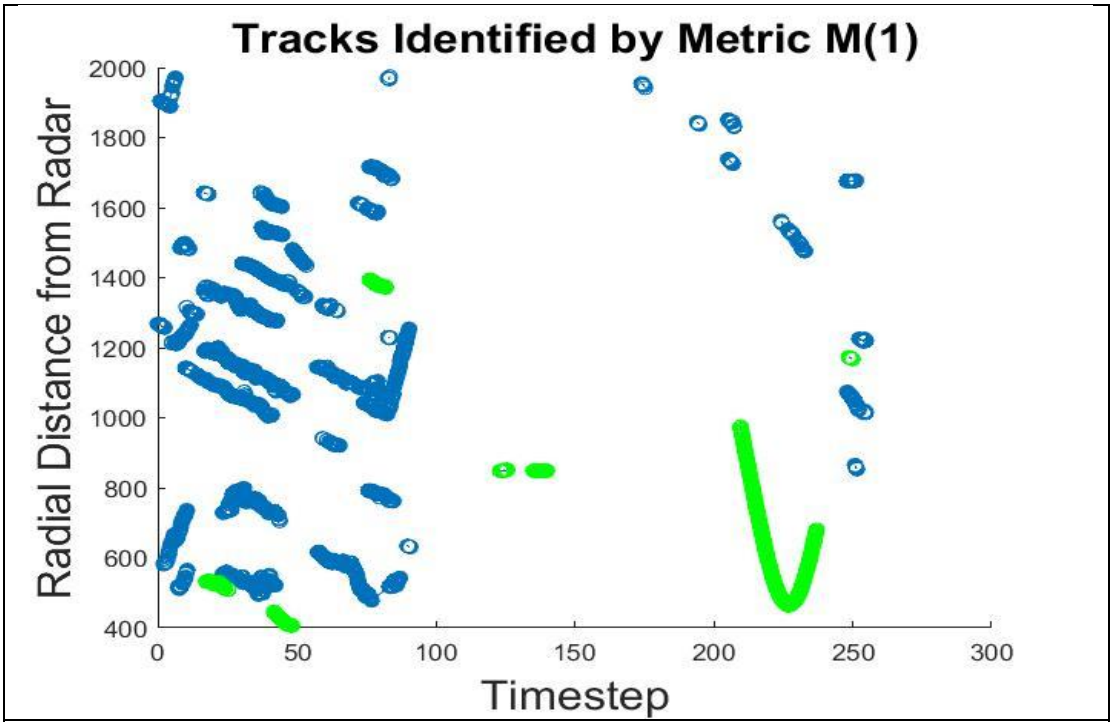

Figure 3: Classification of tracks using the metric M(1) is shown. Tracks with metric value less than a threshold of 0.25 are highlighted in green. The targetship track is identified, but a number of other tracks for slow-moving objects are also identified by the metric.

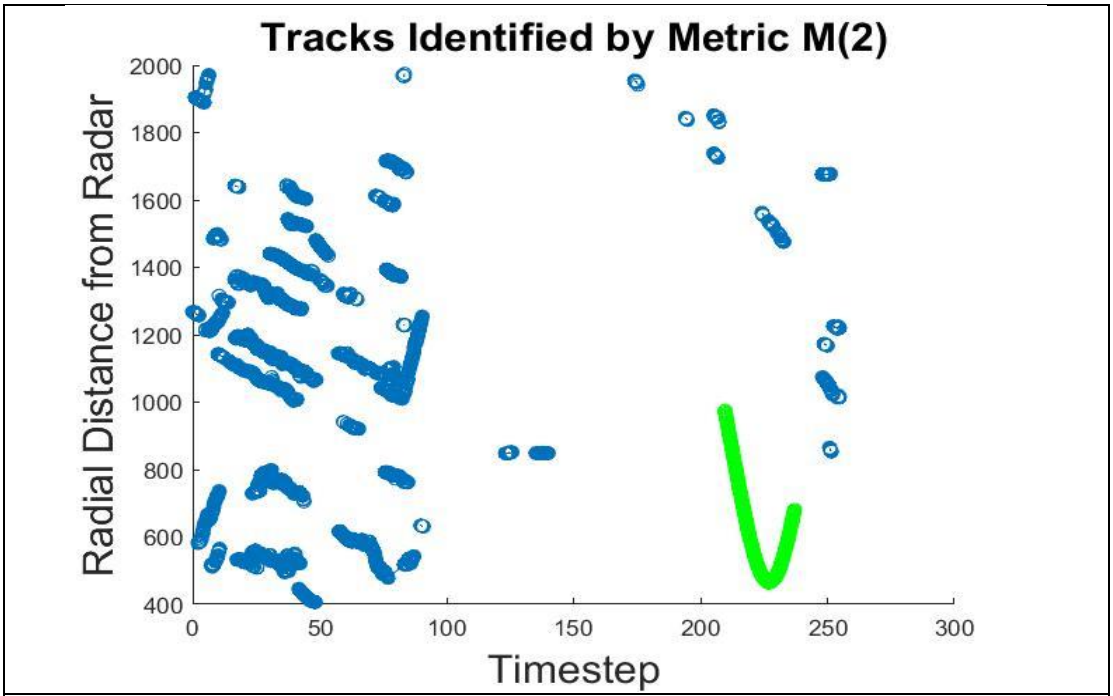

Figure 4: Classification of tracks using the metric M(2) is shown. Tracks with metric value less than a threshold of 0.05 are highlighted in green. The targetship track is exclusively identified in this case. We note that the metrics M(3)-M(5) are also able to perfectly identify the targetship.

Two other analyses were undertaken to assess the usability of the metrics for differentiating aerial objects, focusing on the metric M(2). First, the dependence of the classification performance on the duration of the data used for classification was studied. The metric was found to identify the targetship (i.e., to have smallest value for the track corresponding to the targetship), for all data durations larger than 0.66s. Thus, the metric is seen to be a robust classifier of the targetship track over multiple data durations. Second, the value of the metric M(2) was computed based on 1s data intervals, for different start times during the track. The metric value was found to vary between about 0.035 and 0.075. indicating that the metric remains relatively small (indicating high smoothness) over the duration of track. This consistency in the metric also suggests that it may serve as a relatively robust classifier of aerial object types.

Finally, our analyses of the example data set identified one other possible approach for distinguishing the targetship from other object tracks based on the Fourier transform. In particular, we found that the phase of the frequency response is smooth for the targetship track, as compared to the other tracks. As an illustration, the phase is shown for the targetship track and one other track in Figure 5. We leave it to future work to understand how the phase information can be integrated into a track differentiation algorithm.

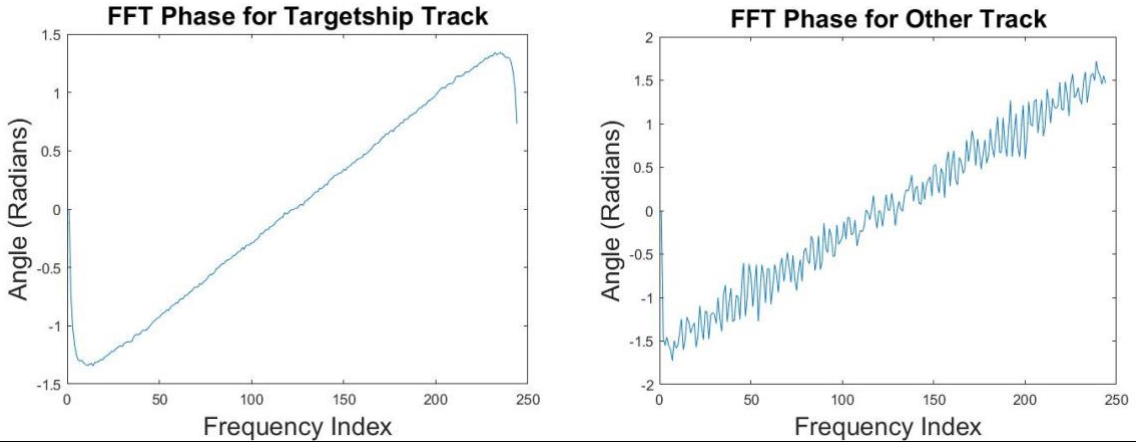

Figure 5: The phase of the Fourier transform for the targetship track and another track are compared. The FFT phase response is smooth for the targetship, while fluctuating substantially for the other track.

V. Performance Analysis of Smoothness-Based Classification

An initial statistical analysis of smoothness-based classification was undertaken, using multiple data sets from the RAAVIN field test. For the statistical analysis, 15 sets of radar track data recorded during a single day of experiments were used for the statistical analysis. The data sets include a total of 20 targetship tracks, where the targetship in each experiment was a small UAS used for the flight test. The data sets also contain 438 other tracks.

We considered the differentiation of targetship tracks from other tracks using the smoothness metric M(2). The metric M(2) was chosen because it was able to differentiate targetship and other tracks for the example data set, while being simple to compute relative to the frequency-response- and polynomial-fitting- based metrics. A histogram of the metric value for the 20 targetship tracks is shown in Figure 6. The metric values for the targetship are seen to range between 0.04 and 0.15, with only one outlier where the metric value was 0.29.

Classification of the tracks based on M(2) using a threshold of 0.15 was considered. For this threshold, targetship tracks were correctly identified with 95% probability (19/20 targetship tracks). Meanwhile, other tracks were misclassified as targetship tracks at a rate of 8.9% (39/438 other tracks). By reducing the threshold to 0.105, the misclassification rate was reduced to 4.6% (20/438 tracks), but at the cost of a reduced targetship identification probability of 85% (17/20 tracks). The analysis indicates that the metric M(2) provides a relatively sensitive and specific test for classification of small UAS tracks. We anticipate that the metrics M(4) and M(5) may also permit effective classification, and expect to assess their performance in future work.

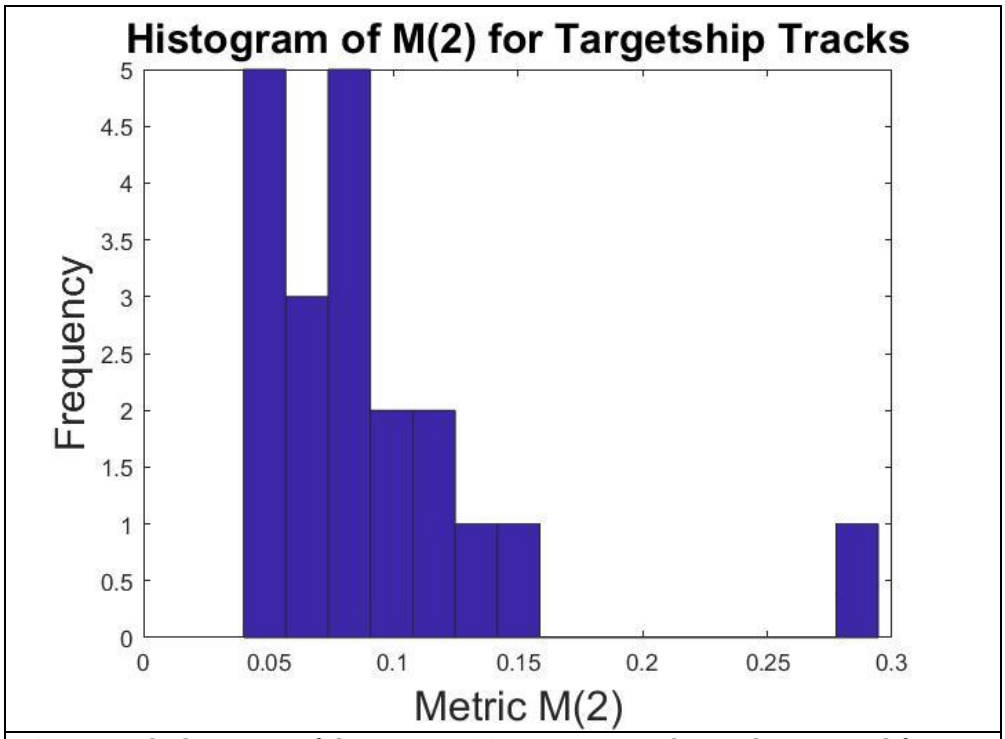

Figure 6: The histogram of the metric M(2) over 20 targetship tracks, extracted from 15 track measurement data sets, is shown. The metric is seen to consistently have a small value between 0.04 and 0.15 over the data sets, with only one outlier track.

VI. Conclusions

The identification of UAS based on the smoothness of measured tracks (trajectories) has been considered. Several metrics for smoothness have been defined, and the metrics have been evaluated using an example data set from the RAAVIN flight test. For the example data sets, the metrics are able to distinguish UAS tracks from other tracks based on their higher smoothness. The metrics can be used even when the UASs are engaged in non-constant-velocity maneuvers. An initial performance assessment was also pursued for one promising metric for smoothness, which is based on the variability in the track's first-difference (derivative) signal relative to its absolute mean, using data from multiple flight tests. The metric achieved good sensitivity and specificity in distinguishing UAS tracks from other tracks. We hypothesize that smoothness metrics used together with other characteristics of ambient UAS flight can differentiate UASs from other aerial objects with even higher precision. Smoothness-based metrics which are able to identify UASs engaged in complex maneuvers may be particularly useful for sense-and-avoid functions in congested or obstructed airspace.

References

[1] Nguyen, Phuc, Mahesh Ravindranatha, Anh Nguyen, Richard Han, and Tam Vu. "Investigating cost-effective rf-based detection of drones." In *Proceedings of the 2nd workshop on micro aerial vehicle networks, systems, and applications for civilian use*, pp. 17-22. 2016.

[2] Lee, Dongkyu, Woong Gyu La, and Hwangnam Kim. "Drone detection and identification system using artificial intelligence." In *2018 International Conference on Information and Communication Technology Convergence (ICTC)*, pp. 1131-1133. IEEE, 2018.

[3] Dolph, Chester, George Szatkowski, Henry Holbrook, Chris Morris, Larry Ticatch, Mahyar R. Malekpour, and Robert McSwain. "Aircraft Classification Using RADAR from small Unmanned Aerial Systems for Scalable Traffic Management Emergency Response Operations." In *AIAA AVIATION 2021 FORUM*, p. 2331. 2021.
[4] Petrizze, David, Kasra Koorehdavoudi, Mengran Xue, and Sandip Roy. "Distinguishing Aerial Intruders from Trajectory Data: A Model-Based Hypothesis-Testing Approach," in *Proceedings of the 2021 American Control Conference*, Online, Jun. 2021.
[5] Petrizze, David, Kasra Koorehdavoudi, Mengran Xue, and Sandip Roy. "Distinguishing Aerial Intruders from Ambient Trajectory Data: Model-Based and Data-Driven Approaches." In *AIAA AVIATION 2021 FORUM*, p. 2332. 2021.
[6] Balasubramanian, Sivakumar, Alejandro Melendez-Calderon, and Etienne Burdet. "A robust and sensitive metric for quantifying movement smoothness." *IEEE transactions on biomedical engineering* 59, no. 8 (2011): 2126-2136.
[7] Consiglio, María, César Muñoz, George Hagen, Anthony Narkawicz, and Swee Balachandran. "ICAROUS: Integrated configurable algorithms for reliable operations of unmanned systems." In *2016 IEEE/AIAA 35th Digital Avionics Systems Conference (DASC)*, pp. 1-5. IEEE, 2016.
[8] Szatkowski, George N., Andrew Kriz, Larry A. Ticatch, Robert Briggs, John Coggin, and Christopher M. Morris. "Airborne radar for sUAS sense and avoid." In *2019 IEEE/AIAA 38th Digital Avionics Systems Conference (DASC)*, pp. 1-8. IEEE, 2019.